Selective excitation of whispering gallery modes in a novel bottle microresonator

Ganapathy Senthil Murugan*, James S. Wilkinson and Michalis N. Zervas

Optoelectronics Research Centre, University of Southampton, Southampton SO17 1BJ, United Kingdom.
smg@orc.soton.ac.uk

Abstract: Selective excitation of spheroidal whispering gallery modes and bottle modes in a robust bottle microresonator fabricated straightforwardly from a short section of optical fiber is demonstrated. Characteristic resonance spectra of long-cavity bottle modes were obtained by using a tapered fiber to excite evanescently bottle microresonator at different points along its axis. Compared to bare-fiber cylindrical resonators, the bottle microresonator results in a 35x increase of the observed Q factor.

OCIS codes: (230.5750) Resonators; (060.2340) Fiber optics components; (140.4780) Optical resonators; (140.3948) Microcavity devices

References and links

1. B. E. Little, J. S. Foresi, G. Steinmeyer, E. R. Thoen, S. T. Chu, H. A. Haus, E. P. Ippen, L. C. Kimerling, and W. Greene, "Ultra-compact Si-SiO2 microring resonator optical channel dropping filters," IEEE Photon. Technol. Lett. **10**, 549-551 (1998).
2. M. Cai, O. Painter, K. J. Vahala, and P. C. Sercel, "Fiber-coupled microsphere laser," Opt. Lett. **25**, 1430-1432 (2000).
3. C.-Yen Chao and L. Jay Guo, "Biochemical sensors based on polymer microrings with sharp asymmetrical resonance," Appl. Phys. Lett. **83**, 1527-1529 (2003).
4. F. C. Blom, D. R. van Dijk, H. J. W. M. Hoekstra, A. Driessen, and Th. J. A. Popma, "Experimental study of integrated-optics microcavity resonators: Toward an all-optical switching device," Appl. Phys. Lett. **71**, 747-749 (1997).
5. W. Klitzing, R. Long, V. S. Ilchenko, J. Hare, and V. Lefèvre-Seguin, "Frequency tuning of the whispering-gallery modes of silica microspheres for cavity quantum electrodynamics and spectroscopy," Opt. Lett. **26**, 166-168 (2001).
6. M. L. Gorodetsky, A. A. Savchenkov, and V. S. Ilchenko, "Ultimate Q of optical microsphere resonators," Opt. Lett. **21**, 453-455 (1996).
7. J.-P. Laine, B. E. Little, D. R. Lim, H. C. Tapalian, L. C. Kimerling, and H. A. Haus, "Microsphere resonator mode characterization by pedestal anti-resonant reflecting waveguide coupler," IEEE Photon. Technol. Lett. **12**, 1004-1006 (2000).
8. G. Senthil Murugan, Y. Panitchob, E. Tull, P. N. Bartlett, J.S. Wilkinson, "Micropositioning of Microsphere Resonators on Planar Optical Waveguides," in Proceedings of Conference on Optics-Photonics Design and Fabrication, Nara, Japan, 7PD2-01 (2006).
9. E. J. Tull, P. N. Bartlett, G. Senthil Murugan, and J. S. Wilkinson, "Manipulating Spheres That Sink: Assembly of Micrometer Sized Glass Spheres for Optical Coupling," Langmuir **25**, 1872-1880 (2009).
10. D. K. Armani, T. J. Kippenberg, S. M. Spillane, and K. J. Vahala, "Ultra-high-Q toroid microcavity on a chip," Nature **421**, 925-928 (2003).
11. M. Sumetsky, "Whispering-gallery-bottle microcavities: the three-dimensional etalon," Opt. Lett. **29**, 8-10 (2004).
12. Y. Louyer, D. Meshede, and A. Rauschenbeutel, "Tunable whispering-gallery-mode resonators for cavity quantum electrodynamics," Phys. Rev. A **72**, 031801(R) (2005).
13. M. L. Gorodetsky and A. E. Fomin, "Geometrical theory of whispering-gallery modes," IEEE J. Sel. Top. Quantum Electron. **12**, 33-39 (2006).
14. G. Kakaranzas, T. E. Dimmick, T. A. Birks, R. Le Roux, and P. St. J. Russell, "Miniature all-fiber devices based on CO_2 laser micro structuring of tapered fibers," Opt. Lett. **26**, 1137-1139 (2001).
15. J. M. Ward, D. G. O'Shea, B. J. Shortt, M. J. Morrissey, K. Deasy, and S. G. Nic Chormaic, "Heat-and-pull rig for fiber taper fabrication," Rev. Sci. Instrum. **77**, 083105 (2006).
16. F. Warken, A. Rauschenbeutel, and T. Bartholomaus, "Fiber pulling profits from precise positioning," Photonics Spectra **42**, 73 (2008).
17. M. Pöllinger, D. O'Shea, F. Warken and A. Rauschenbeutel, "Ultra-high-Q tunable whispering-gallery-mode microresonator," arXiv:0901.4921v1, (2009).

#109918 - $15.00 USD Received 13 Apr 2009; revised 29 May 2009; accepted 9 Jun 2009; published 30 Jun 2009

18. M. N. Zervas, G. Senthil Murugan, and J. S. Wilkinson, "Demonstration of novel high-Q fiber WGM "bottle" microresonators," in IEEE Proc. 10th anniversary International Conference on Transparent Optical Networks **4**, 58-60 (2008).
19. G. Senthil Murugan, J. S. Wilkinson, and M. N. Zervas, "Experimental demonstration of a bottle microresonator," in Conference on Lasers and Electro-Optics 2009, OSA Technical Digest Series (Optical Society of America, 2009), paper JTuD87.
20. G. Chen, Md. M. Mazumder, R. K. Chang, J. C. Swindalt, and W. P. Ackert, "Laser diagnostics for droplet characterization: application of morphology-dependent resonances," Prog. Energy Combust. Sci. **22**, 163-188 (1996).
21. L. Maleki, V.S. Ilchenko, A.A. Savchenkov, and A.B. Matsko, "Crystalline Whispering Gallery Mode Resonators in Optics and Photonics," in *Practical Applications of Microresonators in Optics and Photonics*, A.B. Matsko (ed.) pp. 145-147, CRC Press (2009).
22. B.R. Johnson, "Theory of morphology-dependent resonances: shape resonances and width formulas," J. Opt. Soc. Am. A **10**, 343-352 (1993).
23. J.U Nöckel, "Resonances in nonintegrable open systems," PhD Thesis, pp.92-105, Yale University (1997).
24. S. M. Lacey, "Ray and wave dynamics in three dimensional asymmetric optical resonators," PhD Thesis, pp.141-147, University of Oregon (2003).
25. A. A. Savchenkov, A. A. Matsko, and L. Maleki, "White-light whispering gallery mode resonators," Opt. Lett. **31**, 92-94 (2006).
26. K. J. Vahala, "Optical microcavities," Nature **424**, 839-846 (2003).

1. Introduction

Over the last two decades, microresonators supporting optical whispering-gallery modes (WGMs) have attracted considerable research interest. These resonators confine light both spatially and temporally, resulting in small mode volumes and large optical quality factors (Q), yielding high optical intensities and long photon lifetimes. The combined small mode volume and high Q make them attractive for applications including compact filter elements in optical circuits, narrow linewidth microlasers, biosensors, all-optical switching and cavity quantum electro-dynamics (CQED) [1-5]. However, the mode volume (V) requirements can vary significantly with application, with CQED experiments usually requiring the smallest V, and filters, microlasers and biosensors potentially benefiting from larger-V cavities. Several different microresonator geometries have been reported in the literature each with associated unique characteristics. Microring/disc resonators are convenient for device integration [1]. However, the Q's of such resonators are limited by the surface roughness introduced by the fabrication techniques, such as photolithography and dry etching. On the other hand, while glass microsphere resonators fabricated by melt/re-melt processing may possess record-high Q factors ($\approx 10^{10}$) [6], it is challenging to integrate them fully into optical devices. However, microsphere resonator integration with planar lightwave circuits has been attempted [7-9] with encouraging results. Another widely used and studied WGM microresonator with remarkable performance is the microtoroid [10] with $Q \approx 10^8$.

The whispering gallery mode bottle microresonator was proposed recently and has been studied theoretically [11-13] Double-neck bottle-shaped microresonators have a number of features that distinguish them from equatorial WGM resonators such as microspheres and microtoroids. Bottle resonators are highly oblate resonators and sustain non-degenerate WGMs that exhibit two well-separated spatial regions with enhanced field strength, corresponding to modal turning points. The free spectral range (FSR) of such resonators is predicted to be about one order of magnitude smaller than that of microsphere resonators of equal diameter. This is because bottle microresonators can also be considered as generalized Fabry-Perot cavities where "skew" rays are totally reflected at the two turning points close to the bottle necks. This results in a much longer optical path-length and, therefore, decreased FSR. The reduced FSR is particularly useful when tuning of a high-Q WGM is required to match atomic transition lines in experiments such as CQED [12].

So far, bottle microresonators have been fabricated primarily by "heat-and-pull" techniques, using modified fibre taper rigs [14-16]. A CO_2 laser has been used to heat the fibre locally while it is pulled in a controlled fashion. Early attempts [14,15] resulted, however, in rather poor resonator qualities and measured Q factors of about 3000-4000 [14].

#109918 - $15.00 USD Received 13 Apr 2009; revised 29 May 2009; accepted 9 Jun 2009; published 30 Jun 2009

In order to improve the bottle resonator quality, much more advanced fibre taper rigs have been recently developed utilizing two computer-controlled high precision linear motor stages [16]. This technique produces microbottle resonators in two steps by sequentially micro-tapering the fiber in two adjacent places to form the "bottle". Q factors of about 10^8 have been observed [17].

We have fabricated fiber WGM bottle microresonators from short sections of optical fiber by an alternative simple and versatile "soften-and-compress" technique using a standard fusion splicer to soften the fiber locally [18]. This technique produces robust bottle microresonators in a simple, rapid, single-step process. Fusion splicers are relatively inexpensive pieces of lab equipment with a number of sophisticated heating and motion controls already incorporated. The proposed technique can be modified to include alternative means of local heating, such as CO_2 lasers or fibre micro-heaters. In this paper, we detail the new fabrication technique and present clear experimental evidence of the turning points and the associated intensity maxima of the bottle resonator modes [19]. In addition, we show transmission spectral characteristics when the bottle is evanescently excited at different points along its length. Finally, by fitting the microbottle shape and assigning mode numbers to the transmission resonances, we provide clear physical insight into the observed variation of Q factors as a function of the excitation position.

2. "Soften-and-Compress" microbottle fabrication technique

Fiber splicing is a thermo-mechanical process in which the cleaved ends of two optical fibers are pushed towards each other while they are heated to a temperature at which they soften and fuse together. The heating is usually performed in one of two ways, either by resistive coil (filament) heating or by arc discharge. We have exploited these splicer actions on a piece of *continuous fiber* in order to soften a small region while simultaneously compressing it. These combined splicer actions produce a pronounced bulge along the fiber as shown in Fig. 1(a). The heating method used in the present study was arc discharge with arc duration of about one second. We used multiple short arcs in order to controllably soften the glass. This procedure results in a robust, double-neck bottle fiber microresonator with neck-to-neck distance L_b, bottle diameter D_b and stem diameter D_s. The detailed "bottle" shape is also an important parameter in defining the spectral characteristics and optical properties of the resonator. The shape is defined by the softening temperature profile and the applied compression.

3. Experimental characterization

A tapered fiber with a waist diameter of about 2μm was used to couple light into and out of the bottle resonator. Micro-positioning stages were used to place the tapered fiber on top of, and in close proximity to, the resonator, as close to right angles to the fiber (resonator) axis as obtainable by inspection. A tunable laser source (Agilent 81600B, with tuning range from 1440 to 1640nm) was used to sweep the wavelength and to observe the bottle whispering-gallery-mode resonances. The laser linewidth was 100 kHz and the tuning step interval was 0.1 pm. An infra-red camera was used to image the resonator when excited with the laser. From the obtained images the microbottle dimensions were estimated to be D_s=125μm, D_b=185μm and L_b=400μm (Fig. 1(a)).

The fiber taper was coupled to the bottle resonator at various positions starting from the centre of the bottle to the bottle-neck (furthest turning point) and beyond on both sides. Images of tapered fiber excitation with optical coupling at various positions along the bottle are given in Figs. 1(b)-1(h). The difference in modal intensity distributions for different excitation positions is readily observed from scattering. The images in Figs. 1(d)-1(f) clearly show the excitation of bottle modes with characteristic intensity maxima on both sides of the bottle in the vicinity of the corresponding turning points, in close qualitative agreement with theoretical predictions [11,12]. In contrast, the image in Fig. 1(b) shows the predominant excitation of more conventional quasi-equatorial WGMs similar to those of a highly deformed sphere (spheroid) which, while expected to exist in bottle microresonators, have not been mentioned specifically so far [11,12]. It is important to note that excitation of the bottle modes

#109918 - $15.00 USD Received 13 Apr 2009; revised 29 May 2009; accepted 9 Jun 2009; published 30 Jun 2009

from either side of the bottle produced near-identical scattering intensity patterns with lobes on both sides of the bottle as shown in Figs. 1(e) and 1(h). The scattered intensity patterns of the bottle modes (Figs. 1(b)-1(h)) should be contrasted with that of the perpendicularly-excited normal stripped fiber (Fig. 1(i)), which shows the characteristics of a propagating mode with no axial confinement.

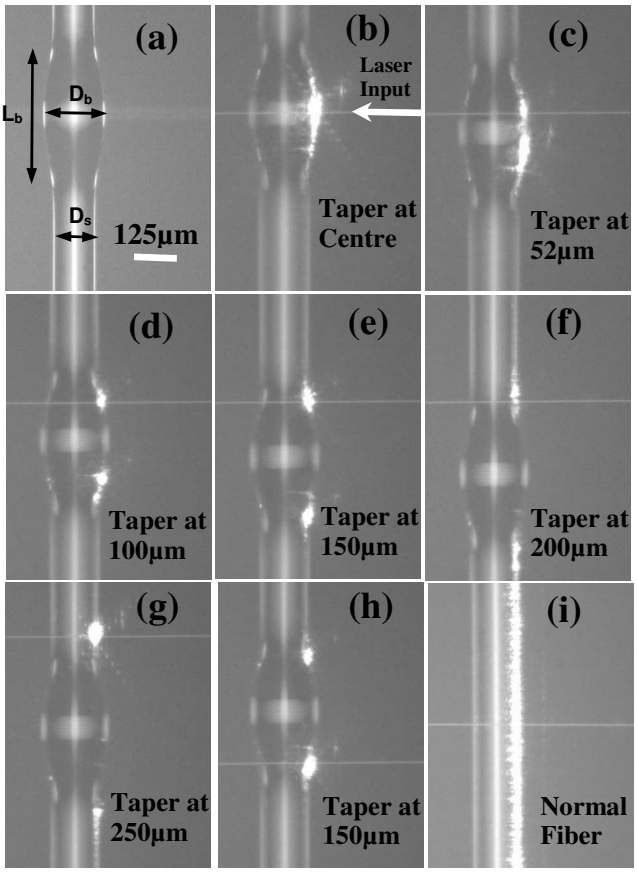

Fig. 1. (a) Optical micrograph of the bottle microresonator coupled to a tapered optical fiber (focus on the bottle), (b) Image of the bottle resonator when the light was coupled through the tapered fiber at the centre (focus on the tapered fiber), (c-g) Image of the bottle resonator when the light was coupled through the tapered fiber at about 52, 100, 150, 200 and 250 µm away from the centre on one side respectively, (h) Image of the bottle resonator when the tapered fiber was at 150 µm on the other side and (i) Image of the tapered fiber coupling to a normal stripped fiber with a cladding diameter of about 125 µm.

Figures 2(a)-2(f) show the resonance spectra of the bottle microresonator when excited at various positions along the bottle. For a given bottle shape, the bottle WGMs (b-WGMs) are uniquely defined by three mode numbers m (azimuthal), p (radial) and q (axial) [11,12] and a corresponding characteristic wavelength λ_{mpq}. Due to the strong asphericity of the bottle resonator, all the supported modes are degenerate with strongly overlapping FSRs and very large mode density [13,20]. The wavelength selectivity and the strength of evanescent excitation of the resonator will depend upon the degree of phase-matching and spatial overlap between the tapered-fiber field and the resonator mode fields at the different positions of the tapered fiber. When the fiber taper is placed near the center of the bottle all the b-WGMs are accessible and can be potentially excited. However, only modes with low q (and large m),

#109918 - $15.00 USD Received 13 Apr 2009; revised 29 May 2009; accepted 9 Jun 2009; published 30 Jun 2009

corresponding to a relatively small separation between turning points, are significantly excited (Figs. 1(b) and 1(c)). Modes with very large q- number show very rapid oscillation of fields around the center of the bottle in the axial direction [12] and are therefore not excited as the field overlap averages to zero. The breaking of degeneracy due to ellipticity results in very dense spectra similar to deformed microspheres [13,20]. The apparent differences in modal density shown in the transmission spectra as the tapered fiber is moved from the bottle centre to the neck is primarily due to differences in modal excitation and selectivity and not inherent modal density changes. Similar effects and differences are observed in the excitation of other types of microresonators, such as spherically-, toroidally- and conically-shaped rim $LiNbO_3$ disks [21].

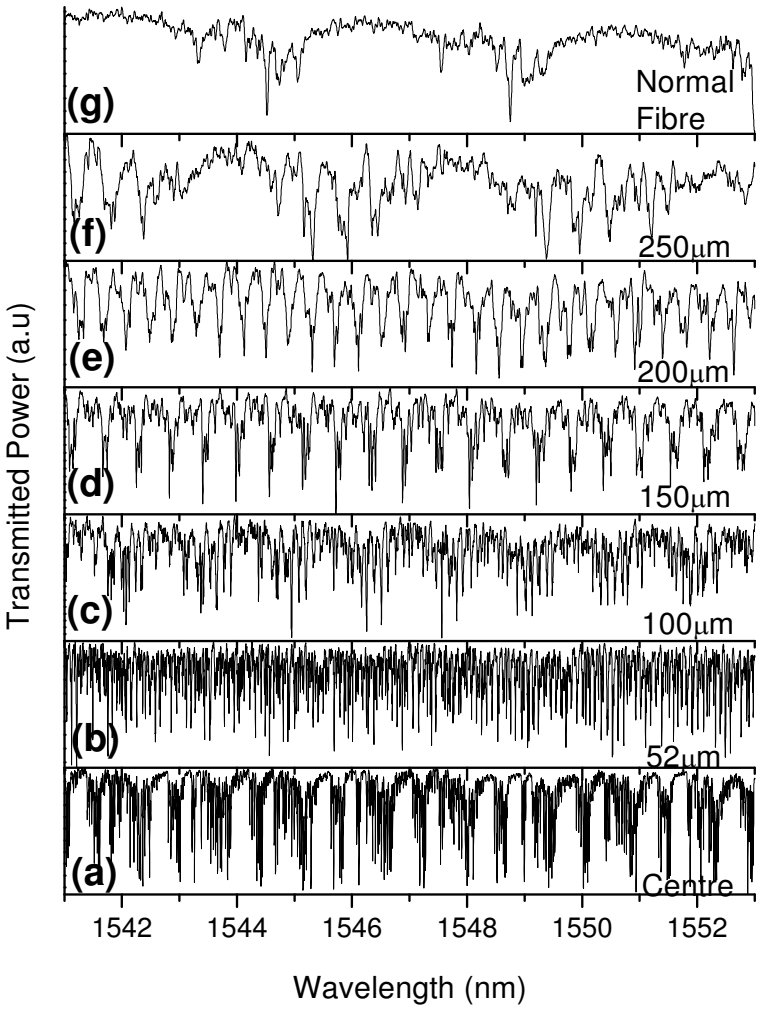

Fig. 2. (a-f) The resonance spectra for the bottle resonator excited using the tapered fiber at the positions shown in Fig 1. (g) The resonance spectrum for a normal stripped fiber with a diameter of 125 μm excited by a tapered fiber normal to it.

Figures 3(a)-3(f) show representative resonant features with the bottle microresonator excited at various places along its length using the tapered fibre. Fig. 3(g) corresponds to the stripped normal fibre stem and it is included for comparison. The wavelength span is varied to best demonstrate the observed Q. In Figs. 3(e)-3(g), adjacent resonances overlap strongly

#109918 - $15.00 USD Received 13 Apr 2009; revised 29 May 2009; accepted 9 Jun 2009; published 30 Jun 2009

due to decreased Q factor. Figs. 3(a)-3(f) also include Lorentzian fits to the measured data in order to calculate the Q of the dominant resonances. The Q-factors as a function of excitation position are plotted in Fig. 4(a) and shown to decrease from $7x10^5$ to $2x10^4$ when the tapered fibre excitation moved from the centre of the bottle to 250μm away from the centre, well beyond the edge of the microbottle. The Q factor of the resonances obtained with the bare normal fiber stem is about $1.9x10^4$. It is shown that the formation of the bottle microresonator results in a more than one order of magnitude, more precisely a factor of 35, increase of the Q-factor compared with the corresponding cylindrical resonator (i.e. bare fiber).

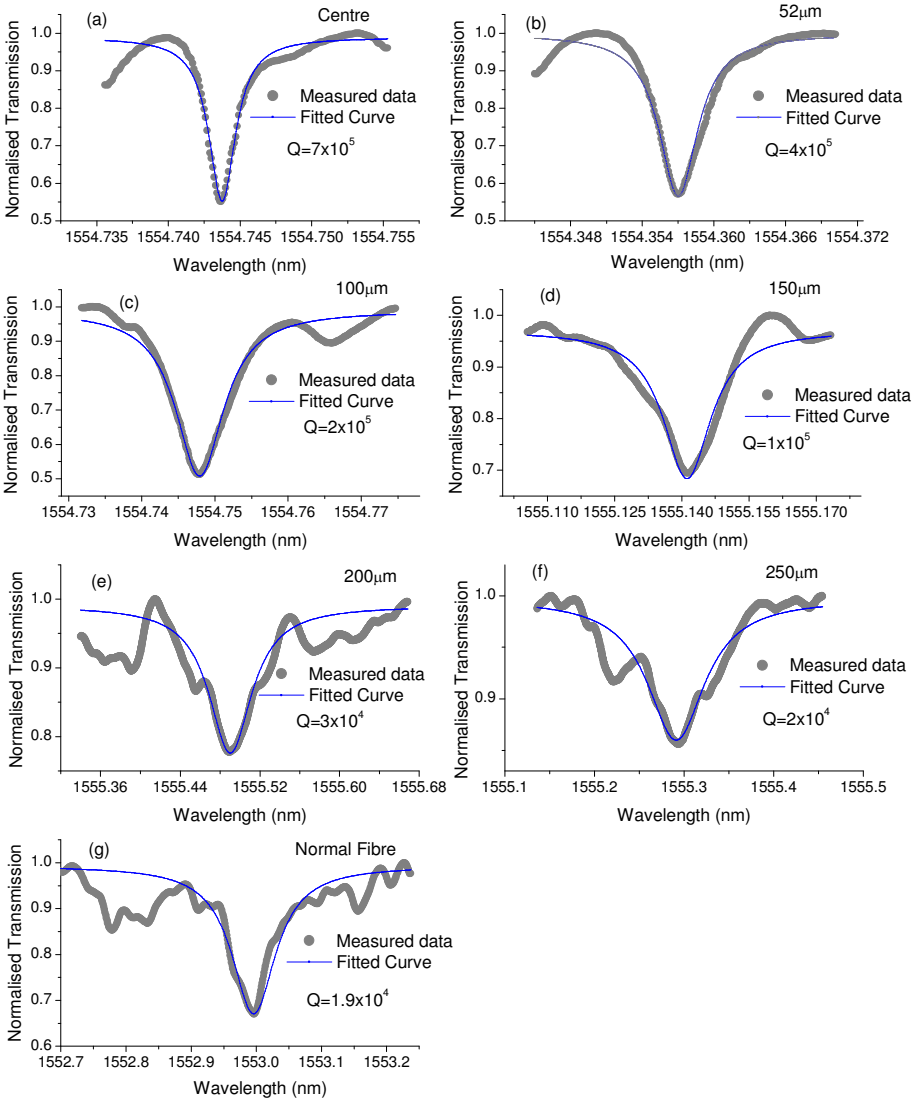

Fig. 3. (a-f) Individual transmission resonances and fitted Lorentzians used for the determination of Q factors of the bottle microresonator, for excitation at the positions shown in Fig. 1. (g) transmission resonance and fitted Lorentzian for bare normal fiber. Transmission is normalized to the local off-resonance transmission.

During the wavelength characterization, it was observed that the maximum transmitted power level was varied with the fiber taper position (not discernible in Fig. 2). In Fig. 4(b), we plot the variation of the average maximum transmission, corresponding to wavelengths

#109918 - $15.00 USD Received 13 Apr 2009; revised 29 May 2009; accepted 9 Jun 2009; published 30 Jun 2009

between resonances (see Fig. 2) as a function of the position of the fiber taper. Comparing Figs. 4(a) and 4(b), it is observed that the Q factor variation shows the same functional relation with the transmission loss. As will be discussed below, the increased losses as the fibre taper is moved along the bottle length, are believed to be due to enhanced leakage into air and into the fibre stems in close proximity to the bottle necks. It should also be noted that there is a marked difference in the variation of both the measured Q factors and the maximum transmission power as the tapered fiber crosses the 200μm point and moves from the outside to well inside the bottle resonator. The Q and transmission loss variation when the tapered fiber is within the bottle resonator shows a strong exponential dependence. In earlier work on bottle resonators with a near-spherical shape, realized using the same technique [18], Q-factors above 10^7 were achieved, showing that the Q-factor here is not limited by scattering or by material absorption but predominantly by leakage into the fibre stems. The design of the optimum bottle resonator profiles which control the extent of this leakage is the subject of further investigation.

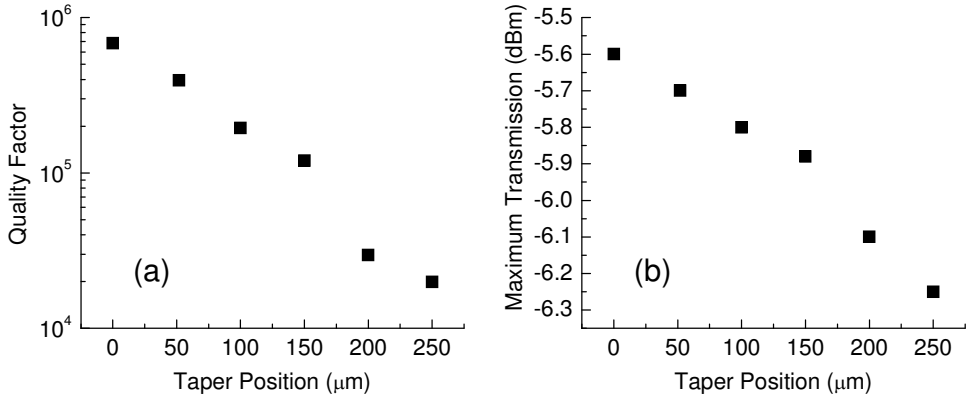

Fig. 4. (a) Q-factors and (b) average maximum transmission as a function of the fiber taper position.

4. Theoretical results

To gain further physical insight into the experimental results, the shape of the bottle microresonator under study was fitted with various shape functions, such as harmonic oscillator, parabolic and cosine profiles. The comparison between harmonic oscillator and parabolic profiles is shown in Fig. 5(a). The cosine profile is not shown as it was almost identical to parabolic. The best fitting function for the outer fiber diameter was found to be the truncated harmonic oscillator profile, namely:

$$D(z) = \begin{cases} D_b \left[1 + (\Delta k\, z)^2\right]^{-1/2} & |z| \le L_b/2 \\ D_s & |z| > L_b/2 \end{cases} \quad (1)$$

with D_b = 185 μm, D_s = 125 μm and Δk = 0.00545 μm^{-1}, as shown in Fig. 5(b). In this case the allowed modal eigenvalues and axial field distributions are given by well known analytical expressions [11,12]. It can be easily shown that the resonant wavelengths and corresponding turning points can be expressed as

$$\lambda_{mq} = 2\pi n_0 \left[\left(\frac{m}{R_b} \right)^2 + \left(q + \frac{1}{2} \right) \Delta E_m \right]^{-1/2} \quad (2)$$

#109918 - $15.00 USD Received 13 Apr 2009; revised 29 May 2009; accepted 9 Jun 2009; published 30 Jun 2009

and

$$z_c = \left[\frac{4}{\Delta E_m}\left(q+\frac{1}{2}\right)\right]^{1/2} \tag{3}$$

respectively, as a function of the mode numbers m and q, where $\Delta E_m = 2m\Delta k/R_b$ and p=1 (R_b=D_b/2). In analogy with quantum-mechanical WKB quantization, the microbottle resonator, in addition to a radial potential (similar to microsphere resonators) [22,23], is characterized by an axial potential given by [11,12] $V(z)=(m/R(z))^2 - (m/R_b)^2$. In the case of harmonic oscillator it takes the form $V(z)=(\Delta E_m z/2)^2$ where $R(z)=(D(z)/2)$, while the total energy is given by $E_{mpq}=k_{mpq}^2 - (m/R_b)^2 = (q+1/2)\Delta E_m$.

For p=1 and effective turning point of about 50μm, from Eqs. (2) and (3) it can be deduced that the corresponding b-WGMs are characterized by q and m mode-numbers around 40 and 535, respectively, with resonant wavelengths in the 1550nm spectral range. On the other hand, when the fiber taper is moved towards the bottle neck (Figs. 1(d)-1(f) and 1(h)), a different sub-set of b-WGMs, with high q-number, relatively low m-number, and widely separated turning points are preferentially excited. The results are summarized in Table 1. It is shown that as the turning point moves towards the bottle neck, the m mode number decreases, while the corresponding q number increases monotonically. Group of b-WGMs with mode numbers in the vicinity of the ones shown in Table 1 show pronounced field maxima around the turning point and are, therefore, expected to overlap strongly with the excitation tapered-fiber beam. Of course, the degree of excitation will also depend critically on the phase-matching conditions.

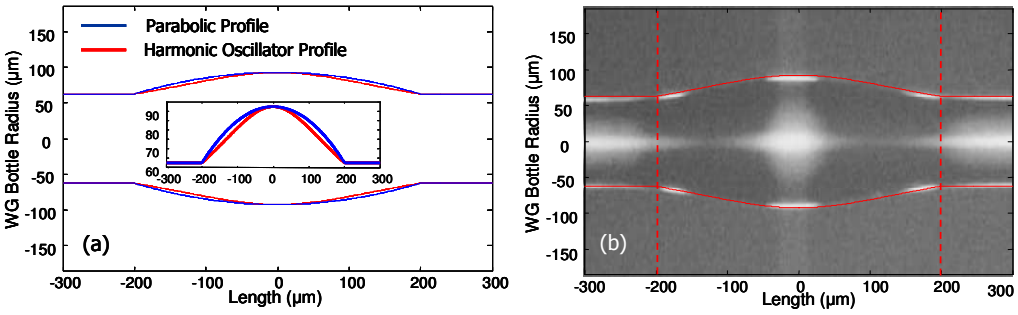

Fig. 5. (a) Harmonic oscillator and parabolic profiles for parameters similar to the experiment. The inset shows a magnified version to visualize the profile differences. (b) The microbottle resonator shown in Fig. 1(a) fitted with truncated harmonic oscillator profile, with D_b = 185 μm, D_s = 125 μm and Δk = 0.00545 μm^{-1}.

Table 1. Azimuthal and axial mode numbers corresponding to different turning points along the bottle axis. The resonant wavelength is around 1550nm and the radial mode number p=1.

Turning Point (μm)	*(m, q)*
20	(550, 6)
50	(535, 40)
150	(430, 285)
200	(375, 440)

Figure 6 shows the potential (solid) and the total energy (dashed) of the b-WGMs corresponding to turning points 50μm (red), 150μm (green) and 200μm (blue). It is shown

#109918 - $15.00 USD Received 13 Apr 2009; revised 29 May 2009; accepted 9 Jun 2009; published 30 Jun 2009

that as the turning point moves closer to the bottle neck, the potential becomes shallower, due to the *m*-number decrease, while the total energy increases, primarily due to the *q*-number increase. As a result, the total mode energy reaches fast the top of the bottle axial potential and, therefore, it becomes easier for the mode to leak into the stems, in the presence of small surface roughness and other irregularities. It is believed that this leakage effect results in the fast, quasi-exponential decrease of the observed Q factors as the excitation point moved closer to the bottle neck. The quasi-exponential dependence of the Q factor on the mode azimuthal number *m* has also been predicted for cylindrical dielectric resonators [23] and microspheres [24].

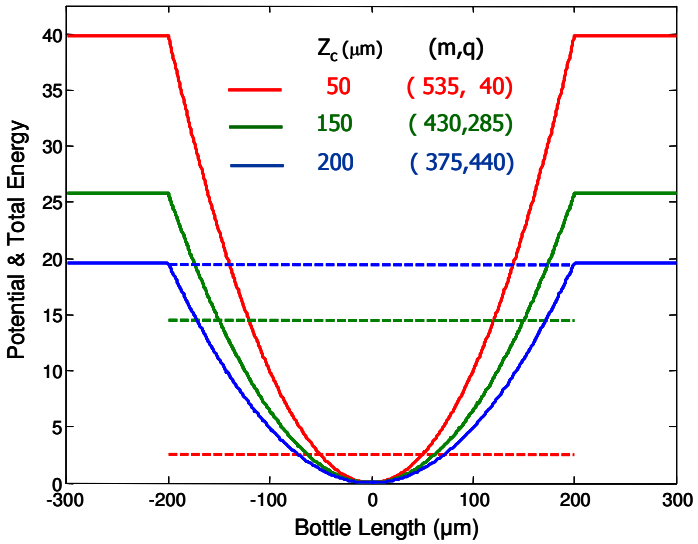

Fig. 6. The potential (solid) and the total energy (dashed) of the b-WGMs corresponding to turning points 50μm (red), 150μm (green) and 200μm (blue).

When the tapered fiber is moved closer to the bottle neck, all the other modes with effective turning points much closer to the bottle center than the current excitation points are not accessible and therefore not excited. This results in seemingly sparser spectra with groups of modes separated by better defined FSR; the groups excited depend upon fibre taper position and hence taper/WGM overlap. As shown in Figs. 2(c)-2(e), the excited modal groups are progressively separated by smaller FSR as the fiber taper moves towards the bottle neck. The FSR observed for the bottle-mode groups in Fig. 2(e) was about 0.4nm near a wavelength of 1550nm, which is about one seventh of the FSR expected for a microsphere with the same diameter (≈185 μm) as the bottle. This FSR is equivalent to that of a standard FP cavity about five times longer than the bottle length, L_b. This increased cavity length is due to the long helical path followed by the bottle mode, travelling back and forth between the two turning points close to the bottle necks. When excitation is attempted beyond these points (Fig 2(f)) only the normal fiber WGMs are excited and an FSR of 4.5nm is observed, in agreement with the WGMs expected in the original fiber of cladding diameter 125 μm (Fig. 2(g)). The full description and assignment of these modes is currently under investigation and the results will be presented in a separate communication.

5. Conclusion

The existence of bottle modes of high axial order (*q* mode number up to 440) with spatially well-separated intensity maxima at the turning points, a characteristic feature of bottle microresonators, has been experimentally demonstrated for the first time. These modes have been selectively excited using a tapered fiber positioned close to the surface of the bottle.

#109918 - $15.00 USD Received 13 Apr 2009; revised 29 May 2009; accepted 9 Jun 2009; published 30 Jun 2009

Previous studies on b-WGM excitation [17] have been limited to q mode numbers of 4. The Q factors of the b-WGMs increased quasi-exponential as the excitation point moved closer to the bottle center. This was shown to be due to the better axial confinement and reduction of the lateral mode leakage. Compared to standard cylindrical resonators, the formation of the bottle microresonator resulted in a 35x improvement of the Q factor, when excited at the bottle centre. The Q factors can be increased further by optimizing the "bottle" shape as well as using higher purity glasses and extra surface treatment, such as chemical or fire polishing, in order to reduce surface roughness and other irregularities.

Free-spectral ranges corresponding to long effective-cavity path lengths have been observed, as expected for bottle modes. The small free-spectral range (FSR) observed is expected to be beneficial in CQED experiments since it requires much lower tuning effort (e.g. mechanical strain) to fully cover the FSR. The pronounced lift of degeneracy and strong spectral overlap of the various mode orders can be quite beneficial in "white-light resonator" applications, such as coherent cavity ringdown [25]. The "soften-and-compress" bottle microresonator fabrication technique has been demonstrated using standard 125μm fibres. However, fibres with smaller diameter, or pre-tapered fibres can be used when larger FSR is required.

Another important microresonator parameter is the mode volume V. Bottle microresonators can show a large range of mode volumes, which can be accurately controlled by the relative position of the excitation fiber micro-taper. The smallest V is achieved when the resonator is excited at the centre (see Fig. 2(b)). At this point V is proportional to the "bottle" waist. On the other hand, large Vs are achieved when the excitation is moved towards the micro-bottle "necks" (see Figs. 2(e)-2(f)). While small V/Q ratios are beneficial for CQED experiments [26], not all photonic applications benefit from small V. For example, when group delay is important, such as in microresonator-based optical delay lines, large-V configurations may be preferable. In addition, compared to microspheres, the b-WGMs occupy a much larger fraction of the resonator volume, and this is expected to improve the output power and efficiency of optically pumped WGM bottle microresonator lasers significantly. Therefore, large-V resonators are potentially advantageous for these applications, and work is underway to demonstrate these features.

Acknowledgements

The authors thank Dr. Yongmin Jung for providing the tapered fiber coupler and Dr. Yuh Tat Cho for providing the fusion splicer. This work was funded by the UK EPSRC under grant GR/S96500/01.

#109918 - $15.00 USD Received 13 Apr 2009; revised 29 May 2009; accepted 9 Jun 2009; published 30 Jun 2009